Supporting Information for

Chlorination of *N*,*N*-dimethylhydrazine compounds: reaction kinetics, mechanisms, and implications for controlling *N*-nitrosodimethylamine formation during ozonation

Woongbae Lee[1], Soyoung Na[1], Changdong Seo[2], Heejong Son[2] and Yunho Lee[1]*

[1]School of Earth Sciences and Environmental Engineering, Gwangju Institute of Science and Technology (GIST), Gwangju, 500-712, Republic of Korea

[2]Busan Water Quality Institute, Gimhae, Gyeongsangnam 621-813, Republic of Korea

*Corresponding author: Yunho Lee: phone: 82-62-715-2468, fax: 82-62-715-2434, email: yhlee42@gist.ac.kr

Submitted to **Environmental Science: Water Research & Technology**

This SI includes 3 texts and 12 figures as supplementary materials, data, and discussion.

SI-Text-1. Standards and Reagents

The following chemicals were obtained from various commercial suppliers and used as received: acetic acid (99.7 %, Sigma), acetonitrile (HPLC grade, Fisher), ammonium chloride (99.5%, Sigma-Aldrich), amoxicillin (Sigma), color reagent for nitrite determination Sulfanilamide / N-(1-Naphthyl)ethylenediamine dihydrochloride solution (Ricca), daminozide (98.0%, Sigma-Aldrich), 1,1-dimethylsemicarbazide (>96%, Tokyo Chemical Industry), 2,4-dinitrophenylhydrazine (97%, Aldrich), formaldehyde dimethylhydrazone (>98%, Tokyo Chemical Industry), formaldehyde solution (36.5-38 % in H_2O, Sigma), glyoxal solution (40 wt. % in H_2O, Sigma), 4,4'-hexamethylenebis(1,1-dimethylsemicarbazide) (>98%, Tokyo Chemical Industry), L-ascorbic acid (reagent grade, Sigma), methanol (HPLC grade, Fisher), methanol-d^3 (99.8%, Sigma-Aldrich), methyl-tert-butylether (HPLC grade, Fisher), methylhydrazine sulfate (>98%, Tokyo Chemical Industry), *N*-(1-naphthyl)-ethylenediamine (≥98 %, Fluka), *N*-nitrosodimethylamine (5000 g/ml in methanol, Supelco) 2,4-pentanedione (99%, Acros), perchloric acid (70 %, Duksan, Korea), phosphoric acid solution (85 wt. % in H_2O, Sigma), potassium iodide (≥99.5 %, Duksan, Korea), sodium acetate (98%, Sigma), sodium azide (≥99.5 %, Sigma), sodium hypochlorite solution (4%, Sigma-Aldrich), sodium phosphate dibasic dehydrate (98.5-101.0%, Sigma), sodium phosphate monobasic dehydrate (≥99%, Sigma), sodium tetraborate decahydrate (≥99.5 %, Sigma), sodium thiosulfate pentahydrate (≥99.5 %, Sigma), sulfanilamide (≥99%, Sigma), and *tert*-butanol (≥99%, Sigma-Aldrich).

SI-Text-2. Determination of second-order rate constants

Chlorination experiments were conducted under pseudo first-order conditions in which FAC was in molar excess to DMZ ($[FAC]_0 \geq 10\times[DMZ]_0$) and the decrease of the concentration of DMZ was measured as a function of time. The reaction was started by injecting an aliquot of a FAC stock solution (~20 mM) to the solutions (20 mL) containing DMZ (2 or 10 μM) in a batch reactor under initial rapid

mixing. At proper time intervals, the reaction solutions (1 mL) were taken and added to a HPLC vials (2 mL) containing 50 μL of a sodium thiosulfate solution (4 mM) to quench the residual FAC. The quenched samples were stored at 4°C before the analysis for the residual DMZ concentration. Ammonia (4 mM) was also tested as the quenching reagent for the residual FAC. The degradation rate of DMZ was not affected by the thiosulfate vs. ammonia quenching reagents (data not shown), indicating that reduction of some initial N-chloro products to the parent compound during the thiosulfate quenching was unlikely.

Figure S1a shows that the decrease of DMZ follows a pseudo first-order (R^2 = 0.95 – 1.0) in the presence of excess FAC ($[FAC]_0$ = 20 – 160 μM), confirming that the reaction is first-order with respect to DMZ. The pseudo first-order rate constants (k_{obs}) could be obtained from the slope of the linear plots of $\ln([DMZ]/[DMZ]_0)$ vs. reaction time at different FAC concentrations. Figure S1b shows the linearity of k_{obs} with respect to FAC concentration ($[FAC]_0$), confirming that the given reaction is also first-order with respect to FAC. From the slope in Figure S1b, the second-order rate constants (k_{app}) for the reaction of DMZ with FAC was determined to be 24 M^{-1} s^{-1} at pH 8. Similar kinetic experiments were carried out with DMZ as a function of pH (4 – 9) in which the k_{app} values were obtained by dividing the k_{obs} values by the FAC concentrations (i.e., $k_{app} = k_{obs} / [FAC]_0$). The same kinetic method was also applied to determine the second-order rate constants for the reaction of DMSC and HDMS with FAC (Figure S2).

Second-order rate constants for the reaction of UDMH with FAC was determined by a competition kinetic method with amoxicillin (AMX). The second-order rate constants for the reaction of FAC with AMX ($k_{FAC\text{-}AMX}$) was 3.80×10^4 M^{-1} s^{-1} at pH 4, 2.10×10^4 M^{-1} s^{-1} at pH 5, 4.67×10^4 M^{-1} s^{-1} at pH 6, 1.19×10^5 M^{-1} s^{-1} at pH 7, 1.39×10^5 M^{-1} s^{-1} at pH 8, and 1.30×10^5 M^{-1} s^{-1} at pH 9.[1] A range of FAC (0 – 60 μM) was added to the solution containing 10 μM of UDMH and 10 μM of AMX at various pHs

(pH 4 – 9). After the reaction was complete (within 1 h), the residual concentration of UDMH and AMX were analyzed. The rate constants ($k_{FAC\text{-}UDMH}$) were obtained from the following Eq. S1:

$$\ln\left(\frac{[UDMH]}{[UDMH]_0}\right) = \frac{k_{FAC-UDMH}}{k_{FAC-AMX}} ln\left(\frac{[AMX]}{[AMX]_0}\right) \quad \text{(S1)}$$

where $k_{FAC\text{-}UDMH}$, $k_{FAC\text{-}AMX}$ represents the apparent second-order rate constant of the reactions of FAC with UDMH and AMX, respectively. Figure S3 shows the representative competition kinetic plot based on Eq. S1 for the reaction of FAC with UDMH vs AMX at pH 7.

Second-order rate constants for the reaction of DMZ with monochloramine (NH_2Cl) was also determined by reacting 1 μM of DMZ with molar excess NH_2Cl (100 – 800 μM). Figure S4 shows the logarithmic relative concentration of DMZ as a function of time during the reaction with NH_2Cl at pH 7. Overall, the degradation of DMZ in the tested NH_2Cl condition (1:800 of $[NH_2Cl]_0$:$[DMZ]_0$) was less than 12% within 2 h, indicating that the reaction is slow with an estimated k_{app} value of ~ 0.02 M^{-1} s^{-1}.

SI-Text-3. Analytical methods

HPLC/UV. Compounds in the concentration range of 0.05 μM –10 μM were determined using a Dionex Ultimate 3000 HPLC system equipped with a UV diode array detector. Separation was achieved by a reverse-phase C18 column (Nucleosil 100-5, Macherey-Nagel, eclipse plus 3.5 μm, 4.6 ×100 mm) using mobile phases consisting of 10 mM phosphoric acid and acetonitrile. UDMH was determined by HPLC analysis of dimethylhydrazone of glyoxal at 305 nm, which was produced from derivatization of UDMH with glyoxal.[2] Prior to HPLC analysis, 1 mL of the sample solutions in 2 mL HPLC vials were mixed with 10 μL of 40 % glyoxal aqueous solution and 20 μL of 1 M phosphate buffer solution adjusted to pH 3.5. After 20 min, the mixture was analyzed by HPLC/UV. MMH was also analyzed as methylhydrazone of glyoxal after the same derivatization procedure used for UDMH. Formaldehyde was determined by HPLC/UV analysis of 2,4-dinitrophenylhydrazone at 365 nm, which

was the product of formaldehyde derivatization with 2,4-dinitrophneylhydrazine.[3] For the derivatization, 850 µL of sample solutions in 2 mL HPLC vials were mixed with 100 µL of a 9 mM solution of 2,4-dinitrophenylhydrazine in acetonitrile and 50 µL of 1 M $HClO_4$ in acetonitrile. After at least 40 min, the mixtures were analyzed by HPLC/UV. Amoxicillin was determined by HPLC/UV analysis at 229nm. Formaldehyde dimethylhydrazone was determined by HPLC/UV analysis at 240 nm within 2 h after samples are prepared due to its instability. NDMA in the concentration range of 0.06 – 10 µM was determined by a HPLC with post-column UV photolysis/Griess reaction detection [4], in which Figure S5a shows the NDMA calibration curve. Limit of detection values for these analyses were: 0.01 µM (UDMH), 0.09 µM (MMH), 0.07 µM (formaldehdyde), 0.04 µM (Amoxicillin), 0.08 µM (formaldehyde dimethylhydrazone-FDMH), and 0.06 µM (NDMA).

HPLC/MS. DMZ, SCA, DMSC, and HDMS were analyzed by HPLC (Alliance 2695, Waters, Milford, MA, USA) equipped with a triple-quadrupole tandem mass spectrometer (Micromass, Waters, Manchester, UK). Separation was conducted by a reversed-phase column (SunFire C18, 2.1 mm × 150 mm, 3.5 µm particle size) using a mobile phase consisting of water and acetonitrile (both containing 0.1% formic acid). The mixture of 10:90 ratios of water and acetonitrile was isocratically eluted. The mass spectrometry was conducted using electrospray ionization (ESI) and multiple reaction monitoring (MRM) for quantification: DMZ (positive ion mode, m/z = 161 → 143), SCA (m/z = 117 → 73), HDMS (m/z = 289 → 61), and DMSC (m/z = 104 → 87). Limit of detection values for these analyses were: 0.04 µM (DMZ), 0.02 µM (SCA), 0.1 µM (HDMS), and 0.2 µM (DMSC).

GC/MS. Methanol was determined by GC (Trace GC Ultra, Thermo Fisher Scientific, USA) equipped with headspace solid-phase microextraction (SPME) autosampler (Triplus RSH™ Autosampler, Thermo Fisher) and a high-resolution MS detector (DFS™ Magnetic Sector GC-High resolution MS, Thermo Fisher). The analytical method was adapted from the literature.[5] 10 mL of the

samples was transferred to the headspace vials (20 mL Crimp top vials, Thermo Fisher) and spiked with 20 mg/L of methanol-d^3 as an internal standard. 1 g of NaCl was added to the samples, and sealed with closure and septa (20mm, 3.2mm thick PTFE, Thermo Fisher). These samples were stored at 4℃ prior to the analysis. A solid-phase micro-extraction (SPME) fiber (60 μm polyethyleneglycol PEG, Supelco) was conditioned in 240℃ for 30 min prior to the first use. The SPME was carried out by incubating the fiber for 15 min at 50℃, and extracting for 15 min at 50℃. The sample injection to the GC was conducted at the inlet temperature of 250℃ in a split mode with 100:1 ratio. The separation was performed by a DB-624 column (60 m (length) × 0.250 mm (ID) × 1.40 μm of film thickness, Agilent technologies, USA) at a flow rate of 1.0 mL/min of helium (99.999% purity, Sinil Gas, Korea) as a carrier gas. The oven temperature program was as follows: 35℃ kept for 3 min, and ramped to 260℃ at 10℃/min; and held for 7 min. The ionization was carried out in electron impact ionization mode (70 eV) at the ion source temperature of 180℃. The mass spectrometry was performed in selected ion monitoring (SIM) mode: m/z of 31 (methanol) and m/z of 34 (methanol-d3) with scanning speed of 2.08 scan per sec. The limit of detection for methanol was 26 μM (= 0.88 mg/L).

NDMA in the ng/L concentration range was determined by GC/MS after solid phase extraction (SPE), following the U.S. EPA-521 method.[6] Coconut charcoal SPE cartridges were conditioned with dichloromethane, followed by consecutive washing with methanol and deionized water before the extraction of samples. Samples were transferred through SPE cartridges at a flow rate of 8−10 mL/min. SPE cartridges were dried by air under vacuum condition for 1 h. The dried cartridges were eluted using 12 mL of dichloromethane under low vacuum condition. The resultant extracted was concentrated in an automated concentration system (TurvoVaps LV Concentration Workstation, Zymark, USA) at 50℃ under nitrogen stream at low pressure, down to 0.25 mL. The injection into the GC was conducted at the inlet temperature of 250℃ in a splitless mode. The separation was performed by a Rtx 5 SIL MS column (30 m × 0.250 mm × 1.0 μm, Restek, USA) at a flow rate of 1.0 mL/min

of helium (99.999% purity, Sinil Gas, Korea) as a carrier gas. The oven temperature program was as follows: 35℃ kept for 6 min; then ramped to 90℃ at 4℃/min; then ramped to 130℃ at 2℃/min, and a final ramp to 260℃ at 10℃/min; Post-run at 290℃ for 2 min. The mass spectrometry was performed in selected ion monitoring (SIM) mode. The selected m/z values were as follows: NDMA (72, 42, 44) and NDMA-d6 (80, 46, 30). Figure S5b shows the NDMA calibration curve, and the limit of quantification for NDMA was 5.0 ng/L.

Identification of volatile transformation products was conducted by using GC (6890A GC, Agilent) equipped with a mass detector (5975C inert MSD with Triple-Axis Detector, Agilent) and a direct injecting autosampler (7693A Autosampler, Agilent), after a liquid-liquid sample extraction to methyl-*tert*-butylether (MTBE). For the extraction, 55 ml of the samples was moved to 65 mL head-space free vials, and 3 mL of MTBE and 10 g of NaCl was added. After a complete dissolution of NaCl, 1 mL of MTBE was delivered to 2 mL of amber vials, and stored at 4℃ prior to the analysis. 1 μL of the extracted MTBE sample was injected to the GC at the inlet temperature of 250℃ in a splitless mode. The separation was performed by a DB-5MS column (30 m × 0.25 mm × 0.25 μm, Agilent) at a flow rate of 1.0 mL/min of helium (99.999% purity, Sinil Gas, Korea) as a carrier gas. The oven temperature program was as follows: 30℃ kept for 2 min; then ramped to 260℃ at 10 ℃/min, and held for 10 min. The mass spectrometry was performed in scan mode with scanned m/z range of 40–250. Identification of products were conducted with the mass spectrum of products based on NIST05 database.

GC/ECD. Trihalomethanes (THMs) were determined by GC (7890A, Agilent) equipped with headspace sampler (7890A, Agilent) and electron capture detector. Chloroform ($CHCl_3$), bromodichloromethane ($CHCl_2Br$), dibromochloromethane ($CHClBr_2$), bromoform ($CHBr_3$) were analyzed. 5 mL of samples were prepared in headspace vials, and spiked with 50 μL of 1.0 mg/L of bromofluorobenzene as an internal standard. An aliquot of the samples was transferred to the GC inlet by the headspace sampler. The temperature of the headspace sampler compartment was set at 70℃,

80℃, and 90℃ for the oven, loop, and transfer line, respectively. The samples were incubated for 15 min and injected for 1 min into inlet at the temperature of 250℃. The injection volume was 3 mL (headspace loop volume) with split ratio of 20:1. The separation was performed by a HP-5MS column (30 m × 0.25 mm (ID) × 0.25 μm, Agilent), with supplying nitrogen gas (99.999%, Sinil Gas, Korea) with a constant flow of 0.6 mL/min. The initial oven temperature was 40℃, which was held for 2 min, and then increased up to 80℃ at the rate of 10℃/min, and maintained for 4 min, and elevated up to 100℃ at the rate of 10℃/min. The post-run sequence was conducted at 310℃ for 2 min. The limit of detection was ~1 μg/L for all four THMs.

Dissolved organic carbon. Dissolved organic carbon (DOC) was determined by a TOC analyzer (Sievers 900 Portable TOC Analyzer). All the vials used in the analysis were pre-cleaned with 2% nitric acid solution for more than one day, and washed with distilled water before use. The limit of detection was 68 μgC/L.

Ion chromatography (IC)/conductivity. IC with conductivity detector (Metrohm Professional IC Vario) was used to determine ammonia and nitrate. Separation was achieved using both of cation and anion exchange column (Metrosep C 4-150/4.0 and Metrosep A Supp 5-150/4.0) with 1.7 mM HNO_3/0.7 mM dipicolinic acid solution (flow rate of 0.9 mL/min) and 3.2 mM Na_2CO_3/1 mM $NaHCO_3$ solution (flow rate of 0.7 mL/min) as the eluents, respectively. Limit of detection values were: 6 μgN/L (or 0.4 μM, ammonium) and 4 μgN/L (or 0.3 μM, nitrate).

UV/Vis absorbance Nitrite was analyzed by UV/Vis spectrophotometer (Evolution 201 UV/vis spectrophotometer, Thermo Fisher) after derivatization using a commercial Griess reagent. 0.12 mL of Griess reagent was added to 3 mL of sample, and the reaction was carried out for 15 min in the dark. Absorbance of the resultant solution was determined at 540 nm by UV-Vis spectrophotometer. The limit of detection of nitrite was 2 μg/L (= 0.14 μM).

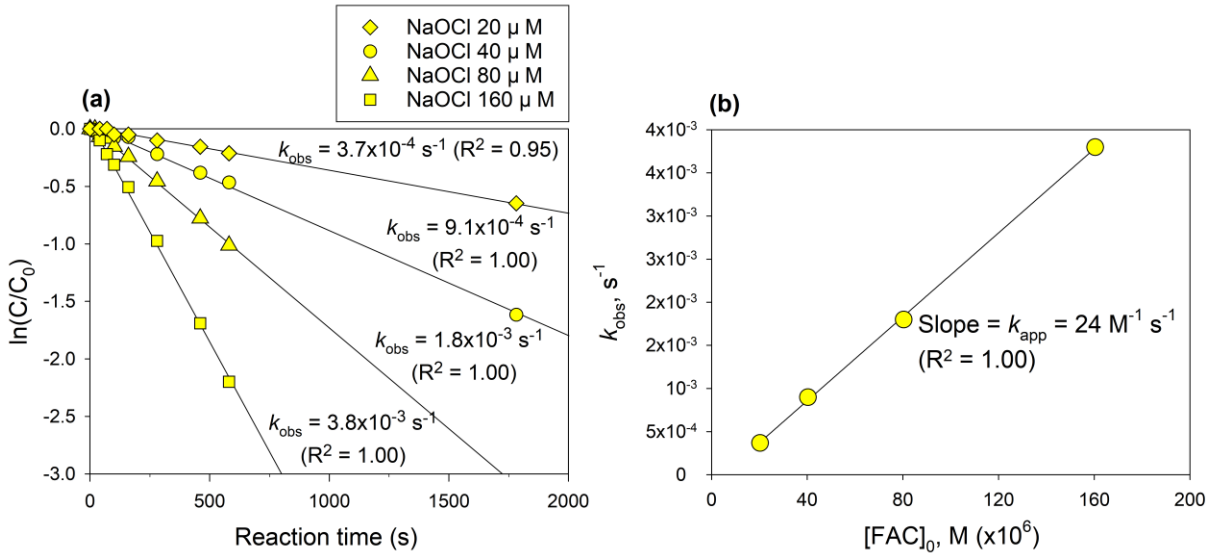

Figure S1. (a) Logarithmic relative concentration of DMZ as a function of reaction time during the reaction of 2 μM of DMZ with an excess of FAC ([FAC]$_0$ = 20, 40, 80, and 160 μM) at pH 8, (b) Observed first-order rate constant (k_{obs}) for the decrease of DMZ vs. the initial FAC concentration at pH 8. All samples were quenched by sodium thiosulfate (0.2 mM), and analyzed for residual DMZ by LC/MS. Symbols represent the measured data and lines represent the linear regressions of the data.

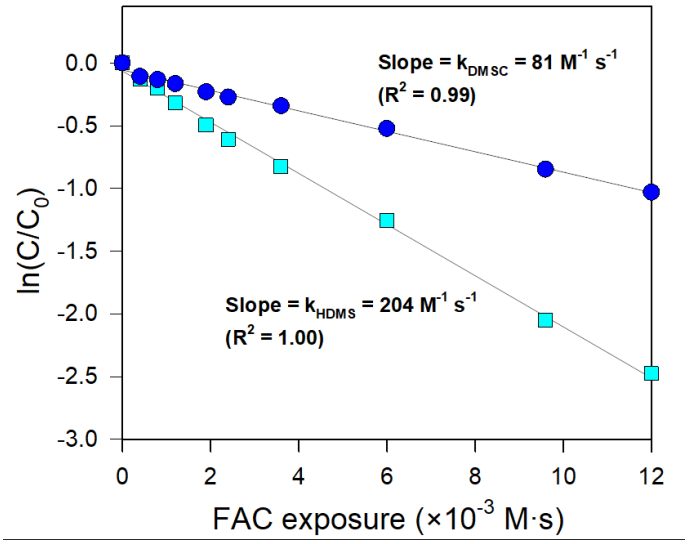

Figure S2. Logarithmic relative concentration of DMSC (circle) and HDMS (square) as a function of FAC exposure at pH 7 (2 mM phosphate buffer). 2 μM of HDMS (or DMSC) was reacted with 20 μM of FAC, and the reaction samples were taken with time and analyzed by LC/MS after the thiosulfate (200 μM) quenching. Symbols represent the measured data and lines have a slope of the second order rate constants of the given reaction. The slopes indicate the second order rate constants of the given reactions.

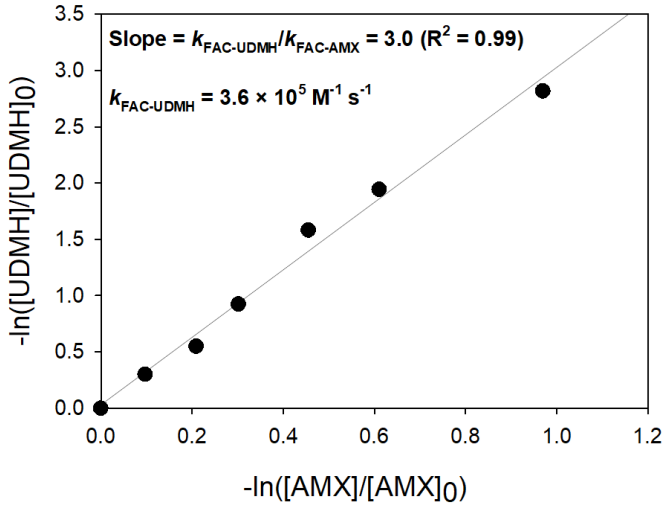

Figure S3. A competition kinetic plot for the logarithmic relative concentrations of UDMH vs. AMX during reaction with FAC at pH 7 (2 mM phosphate buffer). A mixture of 10 μM of UDMH and 10 μM of AMX was reacted with 0 – 30 μM of FAC, and the samples were analyzed for the UDMH and AMX concentrations by LC/UV without the thiosulfate quenching. Symbols are the measured data, and the line represents the linear regression of the data. From the slope of linear regression (= 3.0), the second-order rate constant ($k_{FAC-UDMH}$) for the reaction of FAC with UDMH was determined to be 3.6×10^5 M^{-1} s^{-1} (k for the reaction of FAC with AMX is 1.19×10^5 M^{-1} s^{-1}, Acero et al., 2010).

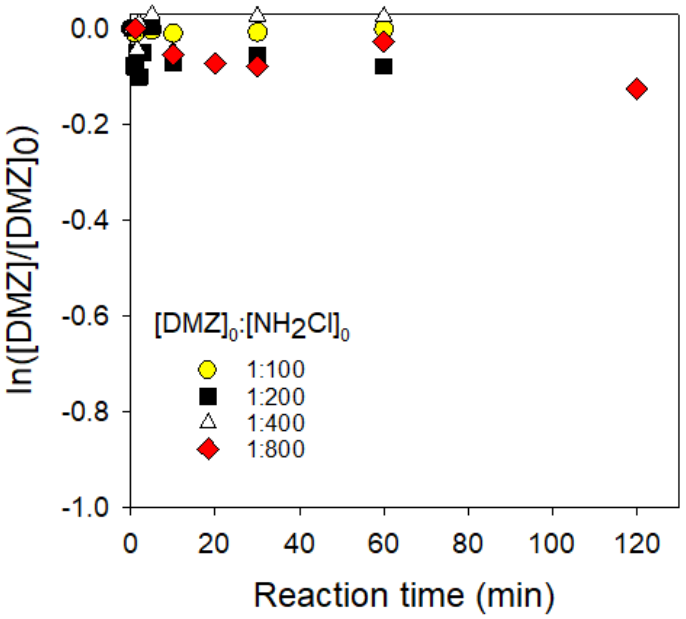

Figure S4. Logarithmic scale relative residual concentration of DMZ during the reaction of DMZ (1 μM) with NH_2Cl (100 – 800 μM) at pH 7 (5 mM phosphate buffer). The reaction samples were analyzed for the DMZ by LC/MS after the thiosulfate quenching (4mM).

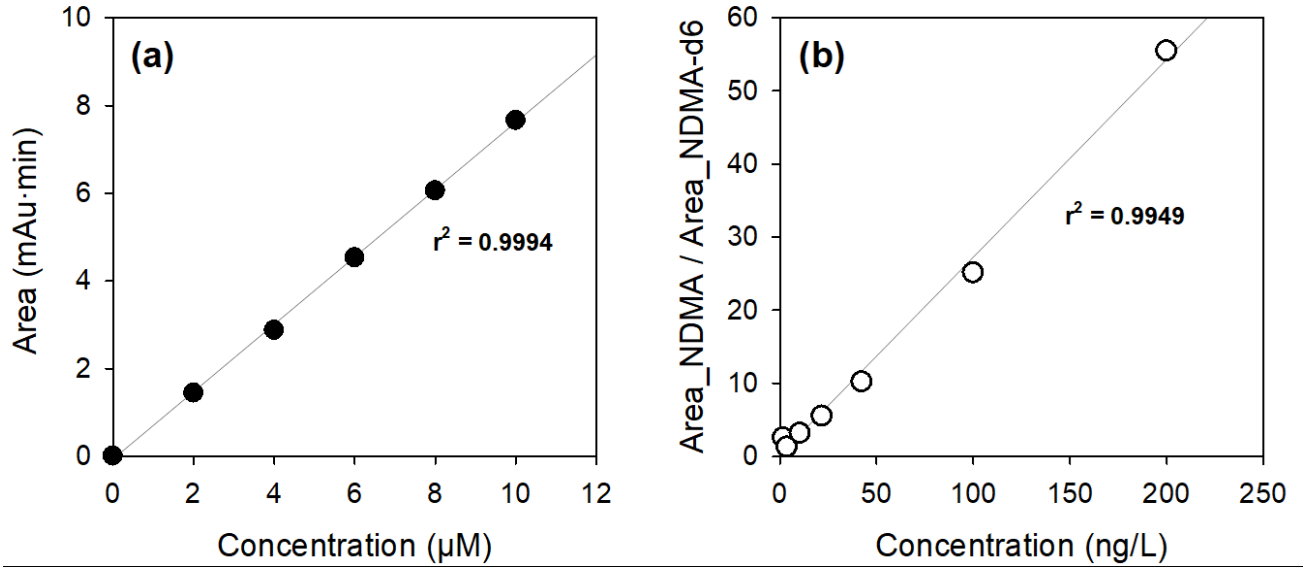

Figure S5. NDMA calibration curves by (a) HPLC with post-column UV photolysis method, and (b) SPE-GC/MS method.

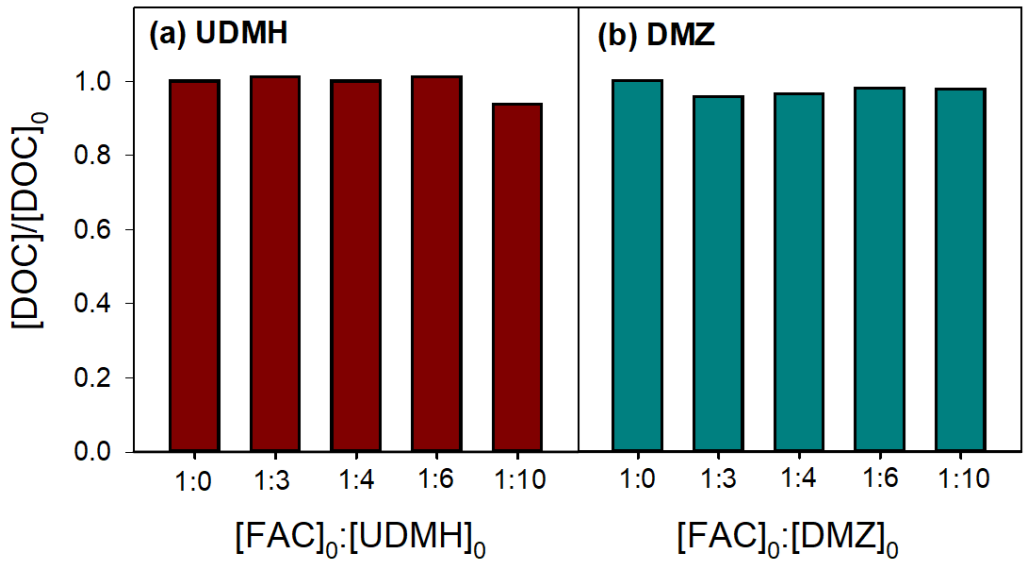

Figure S6. Relative residual concentration of dissolved organic carbon (DOC) after the reaction of (a) UDMH and (b) DMZ with FAC at pH 7 (5 mM phosphate buffer). 50 μM of UDMH or 30 μM of DMZ was reacted with FAC at the molar FAC to the compound ratio ($[FAC]_0/[UDMH]_0$ or $[FAC]_0/[DMZ]_0$ of 1 – 10). After 3 h of the FAC addition, the samples were analyzed for the DOC without the sample quenching. The experiments were conducted duplicate, and the average values were shown.

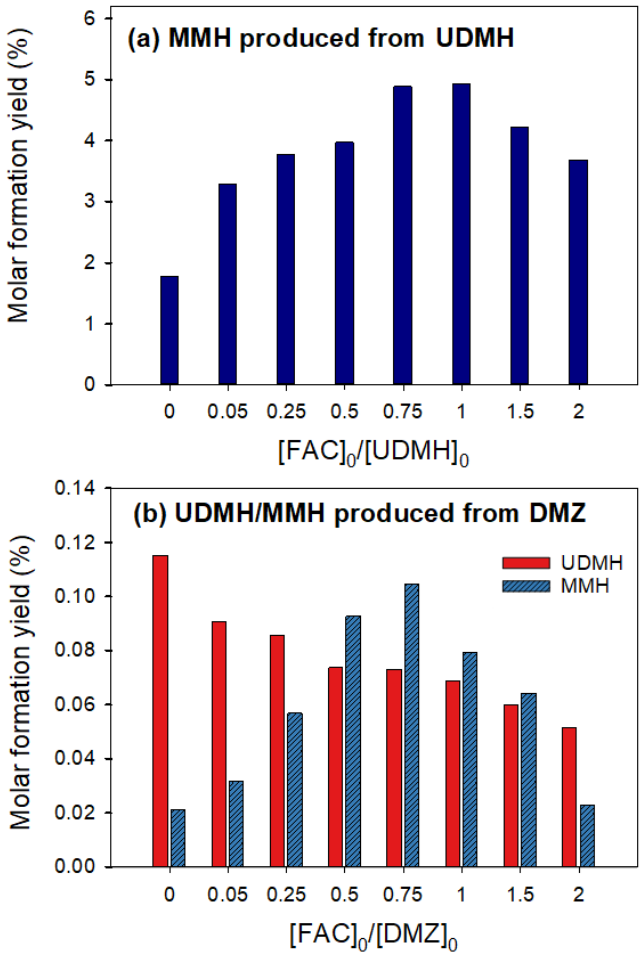

Figure S7. (a) Evolution of MMH during the reaction of UDMH with FAC, and (b) evolution of UDMH and MMH during the reaction of DMZ with FAC. 100 μM of DMZ or UDMH was reacted with 0 – 200 μM of FAC ($[FAC]_0/[UDMH]_0 = [FAC]_0/[DMZ]_0 = 0 – 2$) at pH 7 (5 mM phosphate buffer). After 3 h of the FAC addition, the samples were analyzed for UDMH and MMH by HPLC/UV without the quenching. The experiments were conducted duplicate, and the average values were shown.

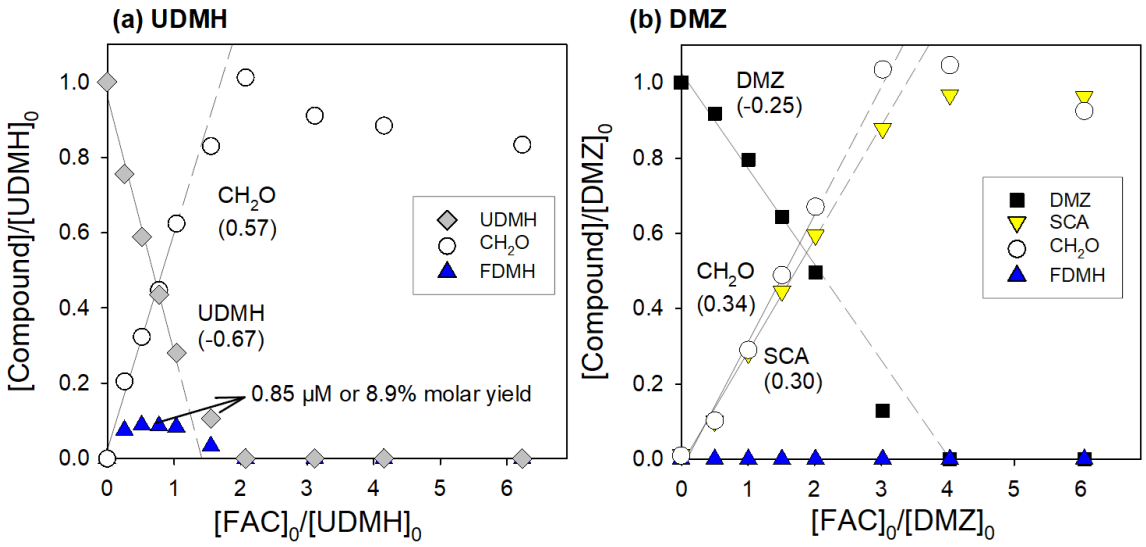

Figure S8. Decrease of (a) UDMH and (b) DMZ, and formation of FDMH, formaldehyde (CH_2O), succinic acid (SCA) after the reaction with FAC at pH 8.5 (5 mM phosphate buffer). 9.6 μM of UDMH or 9.9 μM of DMZ was reacted with a range of initial FAC concentration (0 – 60 μM). After 2 h of the FAC addition, the samples were taken and directly analyzed for FDMH without the quenching. The samples were also stored at 4°C for one day prior to the analysis of DMZ, UDMH, SCA, and CH_2O. Symbol represents the measured data (average value) from duplicate experiments and lines represents the linear regression of the data from the FAC concentration ranges of 0 – 10 μM. The numbers in parentheses indicate the slope of the linear regression.

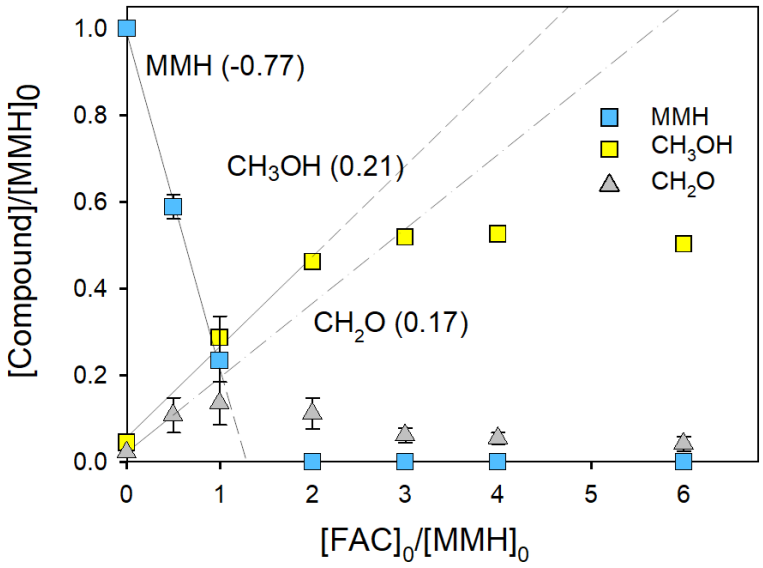

Figure S9. Decrease of MMH and formation of formaldehyde (CH_2O) and methanol (CH_3OH) after the reaction of MMH with FAC at pH 7 (2 mM phosphate buffer). 9.7 μM of MMH was reacted with FAC at the molar ratio of FAC to MMH ($[FAC]_0/[MMH]_0$) of 1 – 6. The experiments for CH_3OH formation were conducted with an initial MMH concentration of 500 μM and initial FAC concentrations of 500 – 3000 μM ($[FAC]_0/[MMH]_0$ = 1 – 6). After 3 h, the samples were analyzed without the sample quenching by HPLC/UV for MMH and CH_2O and GC/MS for CH_3OH. Symbols are the measured data from triplicate (MMH and CH_2O) with error bar and duplicate (CH_3OH) experiments. The lines represent the linear regression of the data from the low FAC concentration range ($[FAC]_0/[MMH]_0$ of 0 – 0.5 for CH_2O, 0 – 1 for MMH, and 0 – 2 for CH_3OH), with the numbers in parentheses showing the slope of the regression.

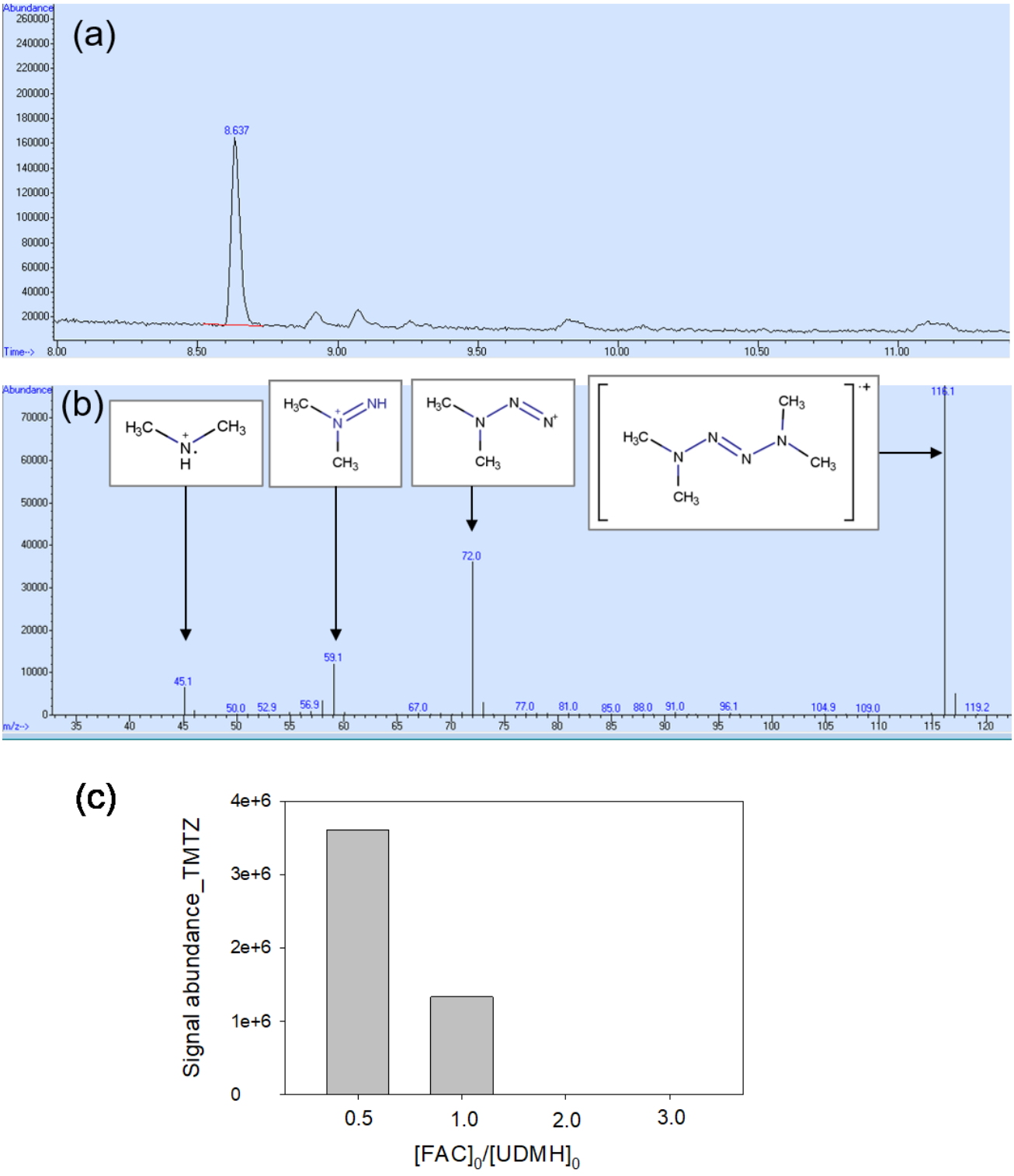

Figure S10. (a) The GC/MS chromatogram and (b) the mass spectrum of the detected peak at RT of 8.6 min of the sample prepared by reacting 100 μM of UDMH with 50 μM of FAC at pH 7 (5 mM phosphate buffer). The detected peak could be identified to be tetramethyltetrazene (TMTZ) based on

the NIST 05 mass spectral library. (c) The evolution of the TMTZ peak area for the samples prepared by reacting 100 μM of UDMH with 50 – 300 μM of FAC ($[FAC]_0/[UDMH]_0 =$ 0.5 – 3). After 3 h of the reaction, the FAC-treated samples were extracted by MTBE for the analysis by GC/MS.

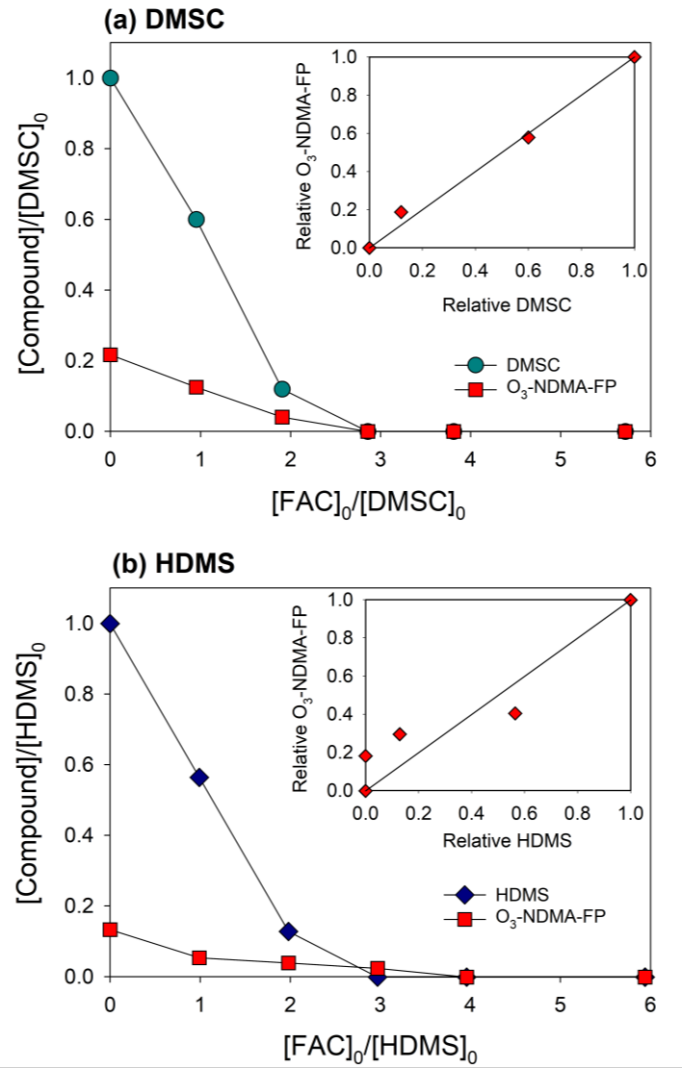

Figure S11. Decrease of (a) DMSC and (b) HDMS and its O_3-NDMA-FP after the reaction of DMSC or HDMS with FAC at pH 7 (2 mM phosphate buffer). 10.5 μM of DMSC (or 10.1 μM of HDMS) was reacted with 0 – 60 μM of FAC ($[FAC]_0/[DMSC]_0$ or $[FAC]_0/[HDMS]_0$ = 1 – 6). After 3 h of the FAC addition, the samples were analyzed for DMSC or HDMS by HPLC/MS without the quenching. The samples were also reacted with 40 μM of ozone for 20 min in the presence of 10 mM *tert*-butanol to determine the O_3-NDMA-FP. Inset figures show the plot of relative DMSC (or HDMS) vs. their relative O_3-NDMA-FP, with a solid line indicating 1:1 correlation. The experiments were conducted duplicate, and the average values were shown.

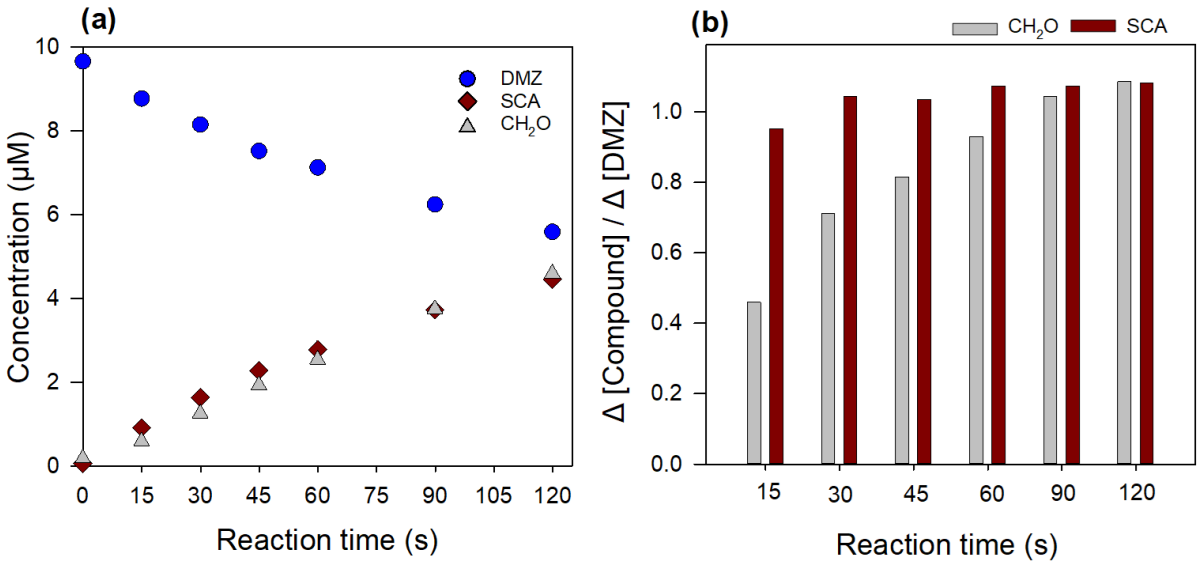

Figure S12. (a) Time-dependent decrease of DMZ and evolution of succinic acid (SCA) and formaldehyde (CH_2O) during the reaction of 9.6 μM of DMZ with 40 μM of FAC at pH 7 (2 mM phosphate buffer), and (b) the relative formation of SCA and CH_2O per consumption of DMZ (=Δ[compound]/Δ[DMZ]) as a function of reaction time. The FAC-treated samples were taken at different times, quenched with thiosulfate (60 μM), and analyzed for DMZ, SCA and CH_2O. The experiments were conducted duplicate, and the average values were shown.

References

1. J. L. Acero, F. J. Benitez, F. J. Real and G. Roldan, Kinetics of aqueous chlorination of some pharmaceuticals and their elimination from water matrices, *Water Res.*, 2010, **44**, 4158-4170.
2. R. Smirnov, A. Smolenkov, T. Bolotnik and O. Shpigun, Precolumn derivatization with glyoxal as a new approach to the highly sensitive HPLC-UV determination of unsymmetrical dimethylhydrazine, *Journal of analytical chemistry*, 2013, **68**, 837-844.
3. F. Lipari and S. Swarin, Determination of formaldehyde and other aldehydes in automobile exhaust with an improved 2, 4-dinitrophenylhydrazine method, *J. Chromatogr. A*, 1982, **247**, 297-306.
4. M. Lee, Y. Lee, F. Soltermann and U. von Gunten, Analysis of N-nitrosamines and other nitro (so) compounds in water by high-performance liquid chromatography with post-column UV photolysis/Griess reaction, *Water Res.*, 2013, **47**, 4893-4903.
5. X. Xu, J. Fillos, K. Ramalingam and A. Rosenthal, Quantitative analysis of methanol in wastewater by GC-MS with direct injection or headspace SPME sample introduction, *Analytical Methods*, 2012, **4**, 3688-3694.
6. J. W. Munch and M. V. Bassett, *METHOD 521: Determination of nitrosamines in drinking water by solid phase extraction and caplillary column gas chromatography with large volume injection and chemical ionization tandem mass spectrometry (MS/MS)*, U.S. Environmental protection agency, 2004.